YMTHE, Volume *31*

Supplemental Information

Targeting long non-coding RNA *NUDT6* enhances smooth muscle cell survival and limits vascular disease progression

Hanna Winter, Greg Winski, Albert Busch, Ekaterina Chernogubova, Francesca Fasolo, Zhiyuan Wu, Alexandra Bäcklund, Bohdan B. Khomtchouk, Derek J. Van Booven, Nadja Sachs, Hans-Henning Eckstein, Ilka Wittig, Reinier A. Boon, Hong Jin, and Lars Maegdefessel

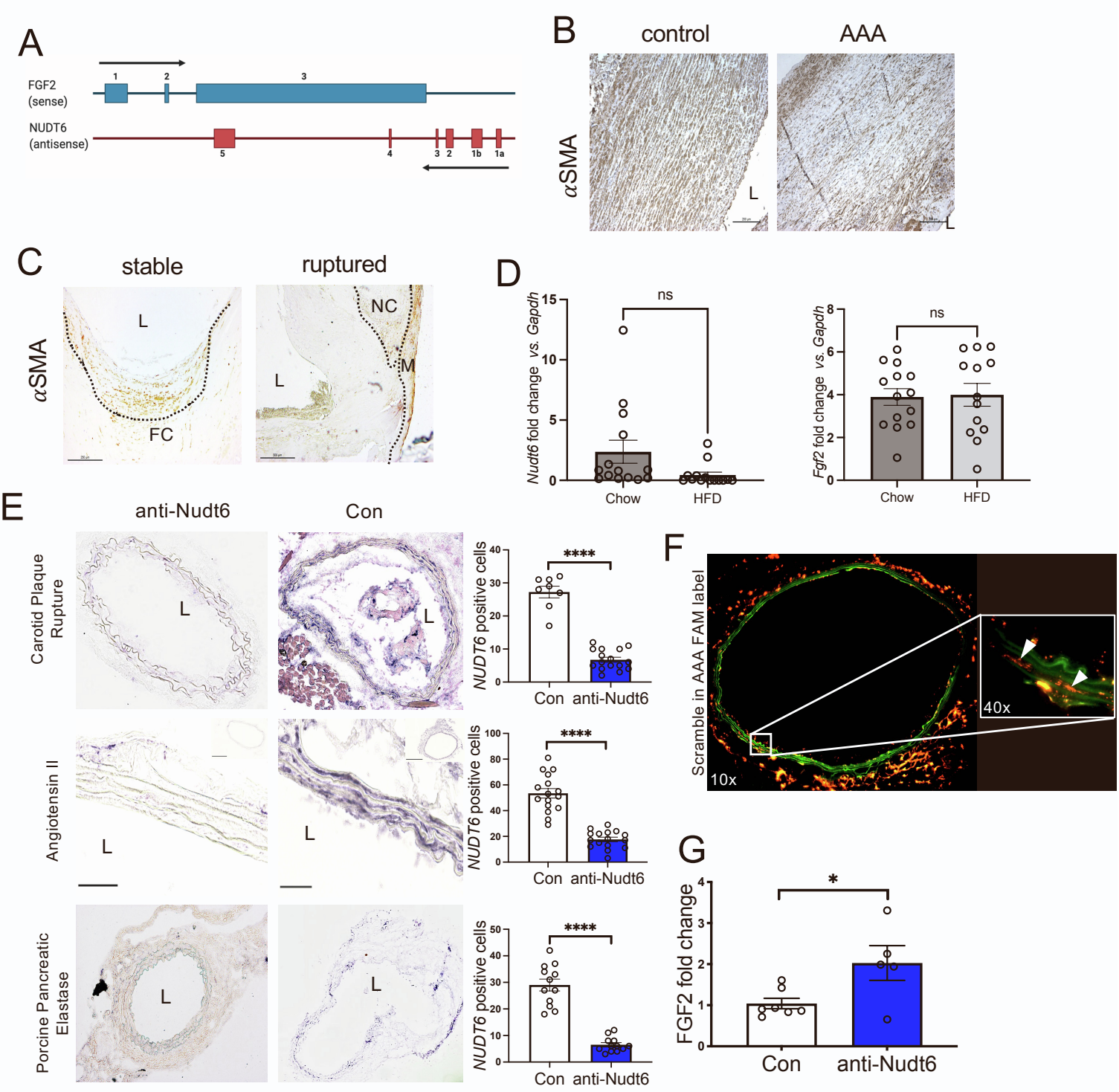

Figure S1

(A) Scheme adapted from [24] showing the common overlap of *NUDT6* and *FGF2* transcripts and respective exons. **(B-C)** Immunohistochemical staining for αSMA of stable and ruptured carotid lesions **(B)** and control aorta and AAA **(C)** show a similar expression pattern compared to FGF2. **(D)** qRT-PCR analysis of aortic arches from *ApoE*$^{-/-}$ mice fed either chow diet or high fat diet (HFD) for 12 weeks show no significant change in *Nudt6* and *Fgf2* expression. **(E)** Confirmatory *In situ* hybridization of Nudt6 in the three mouse models with signal quantification for *Nudt6* signal (4 high power fields per image, N=8-16 counts in total). **(F)** Fluorescent FAM-labelled scramble particles show successful transmission of locked nucleic acid – oligos to the intima media of the abdominal aorta *via* Ultrasound targeted microbubble destruction (UTMD). **(G)** qRT-PCR analysis of abdominal aorta show increased *Fgf2* levels in anti-*Nudt6* treated AngII mice (n=5 per group). Quantitative data are shown as mean + SEM. *p<0.05; ****p<0.0001. Significance is determined using one-tailed Student's t-test.

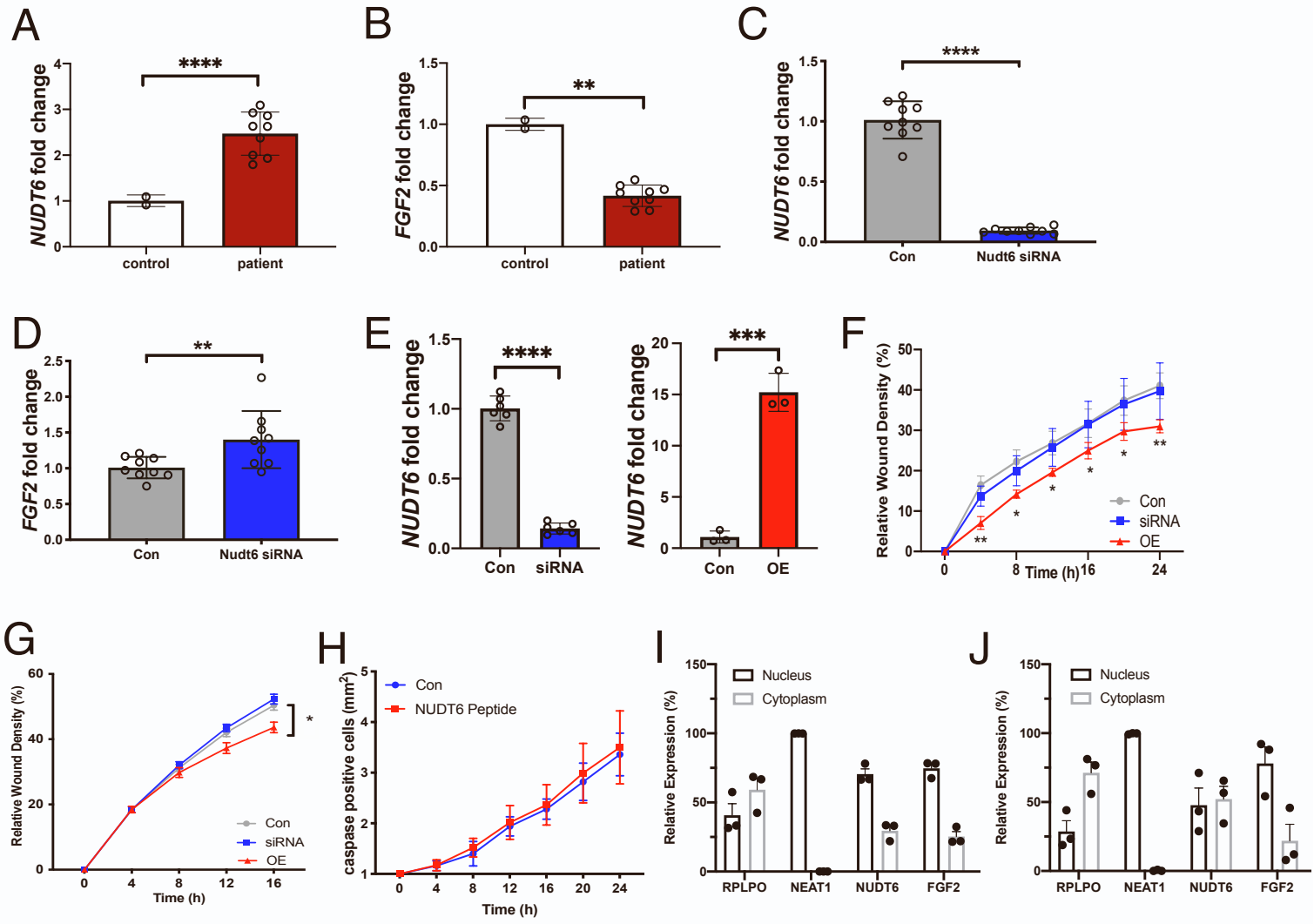

Figure S2

(A-B) *NUDT6* **(A)** and *FGF2* **(B)** mRNA expression after qRT-PCR in 3 different patient-derived aortic VSMCs (n=3 per patient). **(C-D)** Knocking down *NUDT6* via siRNA in patient-derived aortic VSMCs led to a downregulation of *NUDT6* **(C)** mRNA but had a rescuing effect on *FGF2* **(D)** mRNA levels (n=3 per patient). **(E)** Confirmatory qRT-PCR for *NUDT6* after *NUDT6* knockdown and overexpression shows significant deregulation in hAoSMCs (n=6 per group). **(F-G)** Live cell imaging of both hCtSMCs **(F)** and hAoSMCs **(G)** show impaired migratory capacity of cells receiving overexpression vector for *NUDT6*. *NUDT6-siRNA-treated* cells behave as scramble control (n=3 per group). **(H)** Dynamic live-cell imaging of hCtSMCs treated with NUDT6 peptide does not have an effect on apoptosis (n=5 per group). **(I-J)** Nucleocytoplasmic fractionation of hCtSMCs **(I)** and hAoSMCs **(J)** show intracellular distribution of *NUDT6* and *FGF2* compared to nuclear-expressed *NEAT1* and cytoplasmic expressed *RPLPO* (n=3 per group). Quantitative results are shown as mean+SEM. *p<0.05; **p<0.01; ****p<0.0001. Significance was calculated using One-tailed Student's t-test **(A-E, I-J)** or two-way ANOCA with Tukey **(F-H)**.

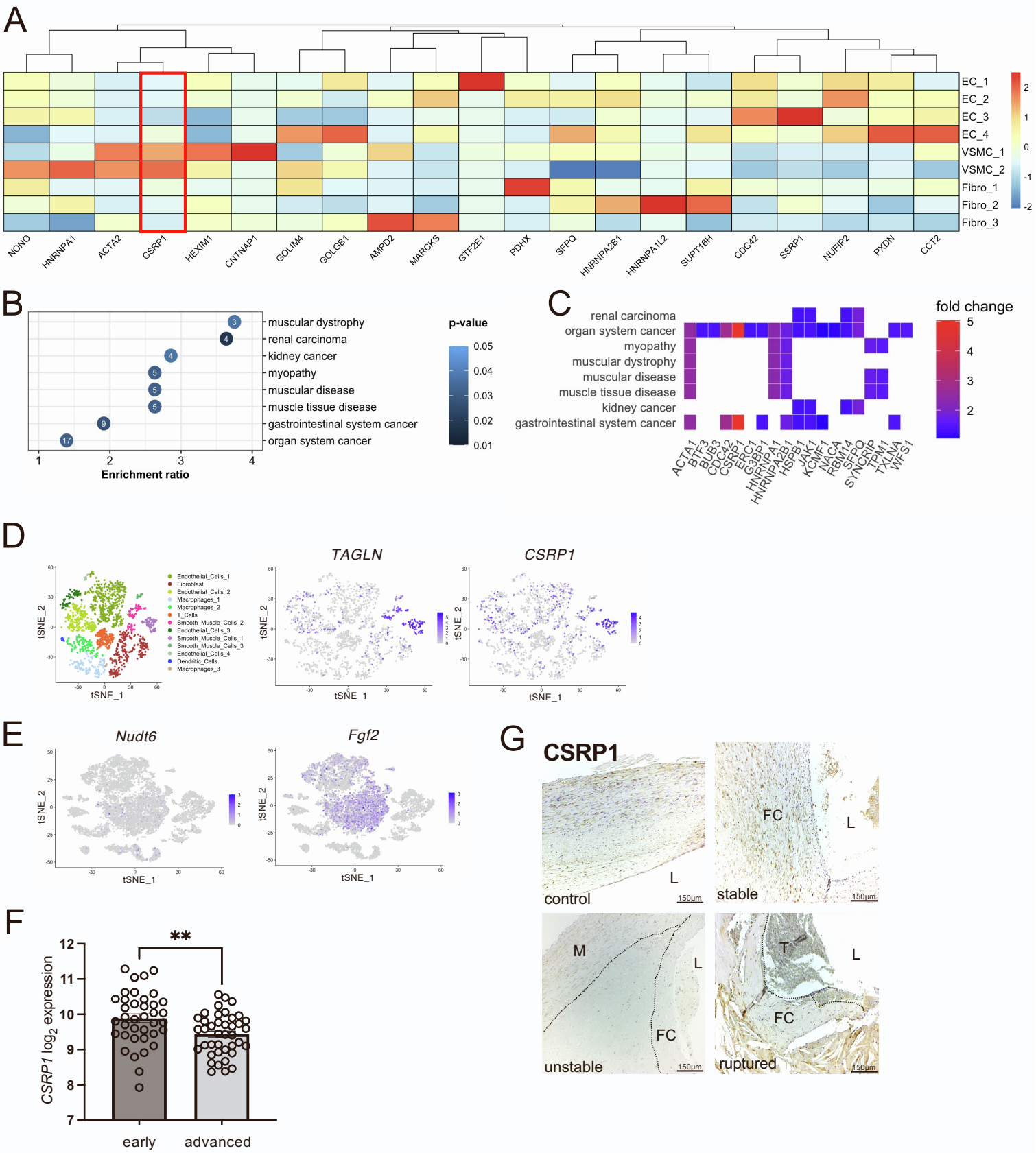

Figure S3

(A) Heat map showing the abundance and expression of CSRP1 in VSMCs and ECs from human single-cell RNA sequencing experiments (Figure 5B). **(B)** Significant enrichment of potential NUDT6:protein interaction partners (Figure 5A) within several Disease Ontology datasets. **(C)** Regulation of potential NUDT6:protein interaction partners within specific Disease Ontology datasets shown in **(B).** **(D)** tSNE plots of scRNA Sequencing data from porcine AAA with expression plots of Transgelin (TAGLN) and CSRP1. AAAs were induced via PPE. **(E)** t-SNE plots of scRNA Sequencing data from murine AAA with expression plots of *Nudt6* and *Fgf2*. **(F)** *CSRP1* expression in early and advanced carotid lesions of a bulk sequencing dataset generated in our lab. **(G)** CSRP1 protein expression in control carotid, stable, unstable and ruptured carotid lesions (L=lumen, M=Media, T=Thrombus, FC=Fibrous Cap). Quantitative data are shown as mean + SEM. **p<0.01; Significance is determined using two-tailed paired Student's t-test.

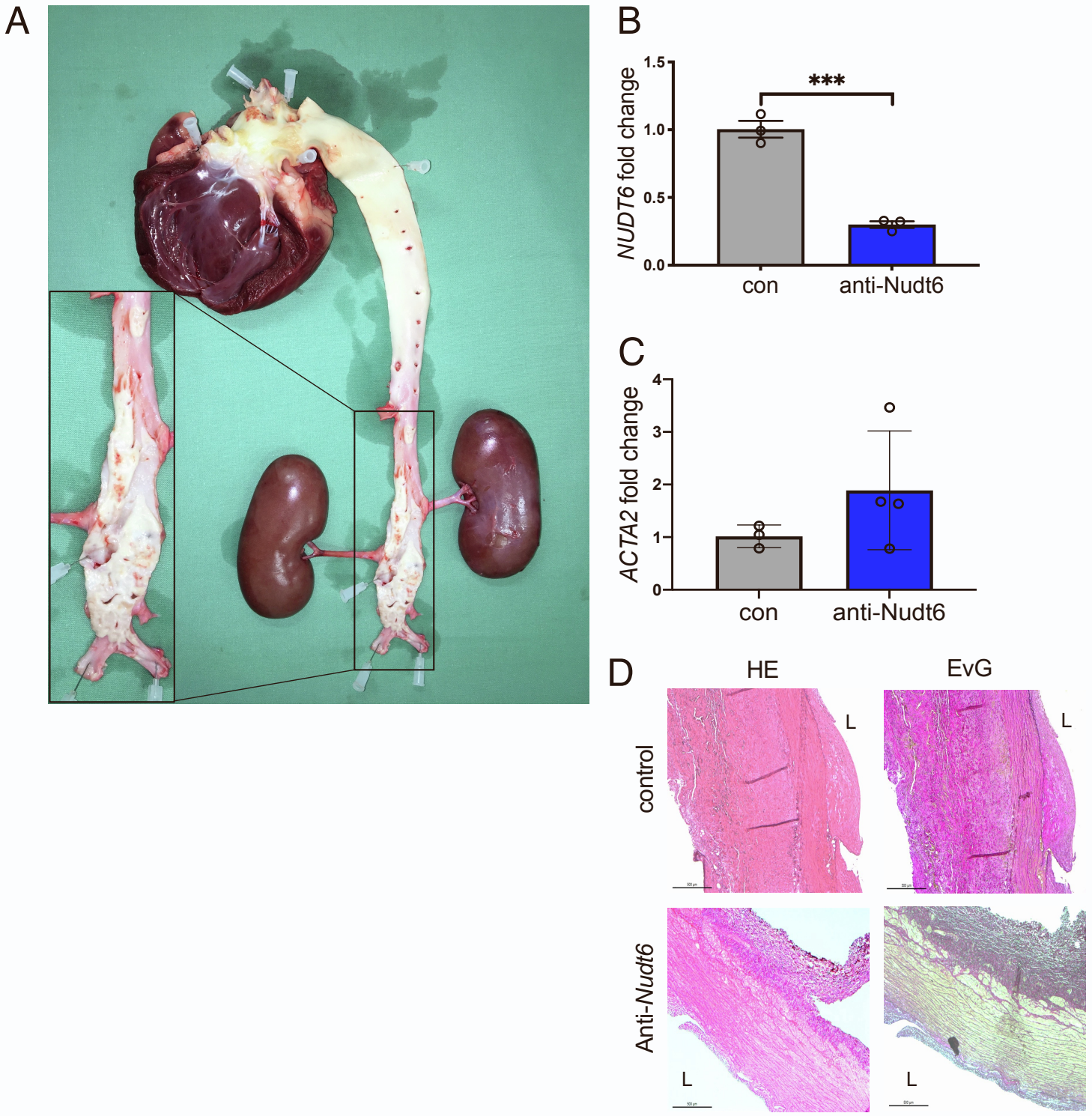

Figure S4

(A) Representative image of the heart, aorta, and kidneys of an LDLR-/- pig with an enlarged image of the abdominal aorta. **(B)** Porcine aortic fibroblasts (n=3) treated with designed porcine *in vivo* locked nucleic acid against *NUDT6* show downregulation of *NUDT6* after treatment. © qRT-PCR of whole porcine aortic tissue (n=3-4) shows an increase in *ACTA2* mRNA. **(D)** HE and EvG stainings of the abdominal aorta anti-*NUDT6* treated (n=4) and control (n=3) animals. Quantitative data are shown as mean + SEM. ***p<0.001. Significance is determined using one-tailed Student's t-test **(B-C)**.

Table S1

Table of the top 20 identified *NUDT6*-RNA Pulldown Targets.

	Protein names	Gene names	Fold enriched *NUDT6* vs CTRL
1	Cysteine and glycine-rich protein 1	**CSRP1**	32.588
2	General transcription factor IIE subunit 1	GTF2E1	11.126
3	Cell division control protein 42 homolog	CDC42	6.958
4	FACT complex subunit SPT16	SUPT16H	5.890
5	Nuclear fragile X mental retardation-interacting protein 2	NUFIP2	5.821
6	Actin, alpha skeletal muscle;Actin, alpha cardiac muscle 1;Actin, gamma-enteric smooth muscle;Actin, aortic smooth muscle	ACTA1;ACTC1;ACTG2; ACTA2	5.646
7	Peroxidasin homolog	PXDN	5.446
8	FACT complex subunit SSRP1	SSRP1	5.404
9	Heterogeneous nuclear ribonucleoprotein A1;	HNRNPA1;HNRNPA1L2	4.940
10	T-complex protein 1 subunit beta	CCT2	4.879
11	Protein HEXIM1	HEXIM1	4.792
12	Non-POU domain-containing octamer-binding protein	NONO	4.729
13	Myristoylated alanine-rich C-kinase substrate	MARCKS	3.975
14	Golgi integral membrane protein 4	GOLIM4	3.930
15	Contactin-associated protein 1	CNTNAP1	3.741
16	AMP deaminase 2	AMPD2	3.662
17	Splicing factor, proline- and glutamine-rich	SFPQ	3.641
18	Heterogeneous nuclear ribonucleoproteins A2/B1	HNRNPA2B1;HNRPA2B1	3.421
19	Golgin subfamily B member 1	GOLGB1	3.384
20	Pyruvate dehydrogenase protein X component, mitochondrial	PDHX	3.331